BULLETIN OF THE CHEMICAL SOCIETY OF JAPAN VOL. 40 85—94 (1967)

Infrared Spectra and Molecular Vibrations of Ethylene Glycol and Deuterated Derivatives

Hiroatsu MATSUURA and Tatsuo MIYAZAWA

Institute for Protein Research, Osaka University, Kita-ku, Osaka

(Received June 21, 1966)

The infrared spectra of ethylene glycol and ethylene glycol-d_2 have been measured in the liquid and crystalline states in the region 4000—300 cm^{-1}. The infrared and Raman spectra suggest that ethylene glycol molecule takes only the gauche conformation as to the C-C bond in both states (the likely models are TGT, TGG and GGG). To establish the vibrational assignments, the normal coordinate treatments of ethylene glycol and its three deuterated derivatives have been carried out for these models by the use of ***GF*** matrix method. The modified Urey-Bradley force field has been used and the force constants have been transferred from similar molecules. The potential energy distributions have also been calculated and the nature of the observed infrared bands and Raman lines in the liquid state has been discussed. The empirical assignments of the methylene rocking modes by the previous investigators have been revised by the present normal coordinate analyses.

The rotational isomerism of ethylene glycol has been studied by the measurements of the dipole moment and vibrational spectra. The dipole moment has been measured in the gaseous[1] and liquid states[2] and in dioxane[3-5] and benzene solutions.[6] The calculated values for various conformations lie within a small range. Therefore, it seems difficult to determine the rotational isomerism from the dipole moment measurements alone.

The rotational isomerism of ethylene glycol has also been studied by the analyses of the vibrational spectra. Kuroda and Kubo[7] have studied the infrared spectra of ethylene glycol and have considered that the trans and gauche forms coexist in the liquid state. White and Lovell[8] have measured the infrared spectra in the solid state and have assigned the bands (900—650 cm^{-1}) to the CH_2 rocking vibrations of the trans and gauche forms. However, Miyake[9] has suggested that liquid ethylene glycol exists predominantly in the gauche form, in comparing the spectrum of ethylene glycol with that of its cobalt or nickel complex. Also, Kanbayashi and Nukada[10] have analyzed the infrared and Raman spectra of ethylene glycol in the gaseous and liquid states and in solution and have concluded that only the gauche form exists for these phases. These spectroscopic studies of the rotational isomerism have all been made by the analyses of the bands observed in the region 1000—700 cm^{-1}. It has been simply assumed that the bands in this region arise only from the CH_2 rocking modes of the trans and/or gauche forms. Undoubtedly, for deriving definite conclusion about the rotational isomerism, it now becomes important to establish the vibrational assignments in this region. Thoughtful normal coordinate treatments will be certainly useful for the analyses of the vibrational spectra.

In the present study, therefore, the normal coordinate treatments were made for various conformations of ethylene glycol and its deuterated derivatives. Also the infrared spectra of ethylene glycol, $HOCH_2CH_2OH$, and ethylene glycol-d_2, $DOCH_2CH_2OD$, in the liquid and crystalline states were measured. For studying the hydrogen bonds in carbon tetrachloride solution, the infrared bands due to the O–H stretching modes were also treated. The infrared spectra of diethylene- through hepta-ethylene glycols and their *O*-deuterated derivatives were also measured in the liquid and crystalline states,[11] and were referred to in the vibrational analyses of ethylene glycol.

The Raman spectra of ethylene glycol in the liquid and crystalline states have been measured previously by Nakamura.[12] The infrared spectra

1) C. T. Zahn, *Physik. Z.*, **33**, 525 (1932).
2) S. R. Phadke, N. L. Phalnikar and B. V. Bhide, *J. Ind. Chem. Soc.*, **22**, 235 (1945).
3) C. P. Smyth, R. W. Dornte and W. S. Walls, *J. Am. Chem. Soc.*, **53**, 2115 (1931).
4) Y. L. Wang, *Z. physik. Chem.*, **B45**, 323 (1940).
5) T. Uchida, Y. Kurita, N. Koizumi and M. Kubo, *J. Polymer Sci.*, **21**, 313 (1956).
6) J. W. Williams, *Z. physik. Chem.*, **A138**, 75 (1928).
7) Y. Kuroda and M. Kubo, *J. Polymer Sci.*, **26**, 323 (1957).
8) H. F. White and C. M. Lovell, *ibid.*, **41**, 369 (1959).
9) A. Miyake, This Bulletin, **32**, 1381 (1959).
10) U. Kanbayashi and K. Nukada, *Nippon Kagaku Zasshi (J. Chem. Soc. Japan, Pure Chem. Sect.)*, **84**, 297 (1963).
11) H. Matsuura and T. Miyazawa, to be published.
12) S. Nakamura, *Nippon Kwagaku Kwaishi (J. Chem. Soc. Japan)*, **60**, 1010 (1939).

of ethylene glycol-d_4, $HOCD_2CD_2OH$, and ethylene glycol-d_6, $DOCD_2CD_2OD$, have been measured by Miyake.[13] These previous results were also used in the present treatments of the normal vibrations and intramolecular force field.

Experimental

The infrared absorption spectra of ethylene glycol and ethylene glycol-d_2 in the liquid state were measured in the region 4000—300 cm^{-1} and the spectra in the crystalline state were measured in the region 4000—400 cm^{-1}. The liquid spectra were measured at room temperature and at 60°C. The crystalline solid films were obtained by slowly cooling the liquid samples down to the liquid nitrogen temperature of 77°K. The solid films were repeatedly annealed until the crystalline spectra were obtained. The infrared spectra in the region 4000—3000 cm^{-1} were also measured for the carbon tetrachloride solutions of ethylene glycol. The solute concentration was varied for studying the effect of the intermolecular hydrogen bonding. The Perkin-Elmer Model 221 Infrared Spectrophotometer equipped with lithium fluoride, sodium chloride or potassium bromide optics and the Model 521 Grating Infrared Spectrophotometer were used for the measurements. The results are shown in Figs. 1—3 and in Tables 1 and 2 together with the Raman data.[10,12]

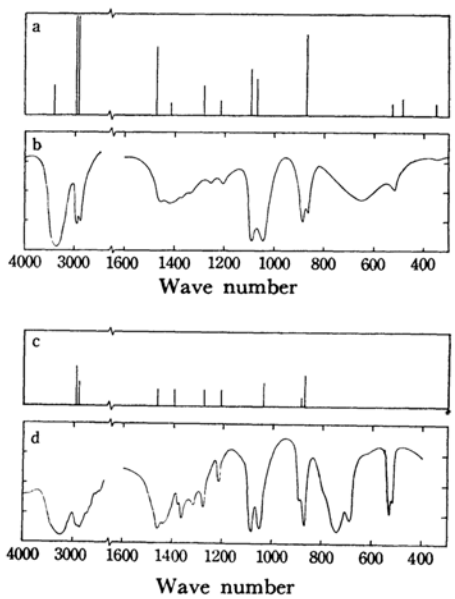

Fig. 1. Raman lines (Refs. 10 and 12) and infrared bands of ethylene glycol, $HOCH_2CH_2OH$, in the liquid (a, b) and crystalline states (c, d).

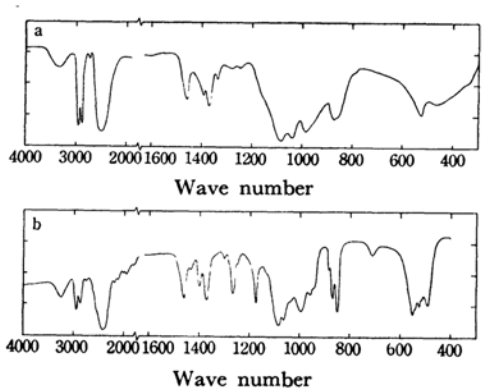

Fig. 2. Infrared bands of ethylene glycol-d_2, $DOCH_2CH_2OD$, in the liquid (a) and crystalline states (b).

13) A. Miyake, *J. Polymer Sci.*, **38**, 497 (1959).

Spectra in the Liquid and Crystalline States

The infrared spectra in the liquid state at 60°C are essentially the same as those measured at room temperature and significant changes in the relative band intensities are not observed. Therefore only the spectra observed at room temperature are shown in Figs. 1 and 2.

TABLE 1. THE INFRARED AND RAMAN FREQUENCIES (IN cm^{-1}) (AND RELATIVE INTENSITIES[a]) OF ETHYLENE GLYCOL, $HOCH_2CH_2OH$, IN THE LIQUID AND CRYSTALLINE STATES

Liquid			Crystalline	
Infrared	Raman[b]	Raman[c]	Infrared	Raman[b]
3353 (vs)	3350 (vs)	3368 (m)	3225 (vs)	
2941 (s)	2945 (s)	2935 (vs, DP)	2924 (s)	2935 (s)
2876 (s)	2878 (s)	2880 (vs, P)	2865 (s)	2880 (m)
1459 (m)	1462 (s)	1462 (s, DP)	1460 (m)	1460 (w)
1414 (m)		1405 (w)	1437 (m)	
1392 (sh)				1391 (w)
1370 (m)			1377 (w)	
			1362 (m)	
1333 (m)			1314 (m)	
	1289 (m)			
	1268 (m)	1272 (m,DP)	1277 (m)	1273 (w)
1255 (w)				
1205 (w)	1208 (w)	1209 (w)	1212 (w)	1208 (w)
1087 (s)	1089 (m)	1088 (m, P)	1081 (s)	
	1062 (m)	1062 (m, DP)		
1043 (s)	1040 (m)		1050 (s)	1039 (m)
883 (s)	890 (m)		887 (m)	888 (w)
862 (s)	862 (s)	864 (s, P)	870 (s)	872 (m)
			737 (s)	
650 (m)			689 (s)	
517 (m)	523 (w)	524 (w, DP)	527 (m)	
			520 (m)	
	480 (w)	482 (w, P)		
345 (w)	349 (w)	350 (w)		

a) vs, very strong; s, strong; m, medium; w, weak; sh, shoulder; P, polarized; and DP, depolarized.
b) Ref. 12.
c) Ref. 10.

Table 2. The infrared frequencies (in cm^{-1}) (and relative intensities[a]) of ethylene glycol-d_2, $DOCH_2CH_2OD$, in the liquid and crystalline states

Liquid	Crystalline
2938 (s)	2943 (s)
2877 (s)	2873 (s)
2475 (vs)	2405 (vs)
1460 (m)	1463 (m)
	1437 (w)
1390 (m)	1401 (m)
1371 (m)	1372 (m)
1335 (w)	1302 (w)
1279 (w)	1267 (m)
1247 (w)	1250 (sh)
1155 (sh)	1174 (m)
1085 (s)	1083 (s)
1037 (s)	1065 (s)
	1037 (m)
985 (s)	994 (s)
950 (sh)	959 (m)
	944 (sh)
	884 (w)
877 (s)	870 (m)
862 (s)	850 (s)
520 (m)	551 (s)
	527 (s)
465 (m)	491 (s)
340 (w)	

a) See a) of Table 1.

For liquid or crystalline ethylene glycol, $HOCH_2CH_2OH$ (Fig. 1), the infrared bands and the Raman lines are observed at nearly the same frequencies; that is there is no indication of the presence of any centrosymmetrical forms which should obey the rule of mutual exclusion for the infrared and Raman frequencies.

The frequencies of the infrared bands and the Raman lines observed in the liquid state are listed together in Table 1. The strong infrared band and the Raman line at about 3350 cm^{-1} are undoubtedly due to the O–H stretching mode. The infrared bands at 2941 and 2876 cm^{-1} and the corresponding Raman lines are assigned to the stretching modes of the CH_2 groups. The medium infrared band observed at 1459 cm^{-1} corresponds to the strong Raman line at 1462 cm^{-1}. The broad infrared band at 1414 cm^{-1} is observed together with shoulders at 1392 and 1370 cm^{-1}, and a Raman line is observed at 1405 cm^{-1}. In the region 1100—1000 cm^{-1}, two strong bands are observed at 1087 and 1043 cm^{-1}, corresponding to the Raman lines at 1088 and 1040 cm^{-1}, respectively, but no infrared peak is resolved at the Raman frequency of 1062 cm^{-1}. The infrared bands at 883 and 862 cm^{-1} obviously correspond to the Raman lines at 890 and 864 cm^{-1}, respectively.

The very broad band near 650 cm^{-1} disappears on *O*-deuteration and the corresponding band is located near 465 cm^{-1} for the deuterated derivative. Therefore, the band at 650 cm^{-1} is now assigned definitely to the torsional mode of the O–H group or, in other words, to the internal rotation mode about the C–O bond. The infrared bands at 517 and 345 cm^{-1} and the Raman lines at 524 and 350 cm^{-1} are due to the skeletal deformation modes. A Raman line is observed at 482 cm^{-1}, but the corresponding peak is not observed in the infrared absorption.

The infrared and Raman frequencies of $HOCH_2CH_2OH$ in the crystalline state are also listed in Table 1. In the region 1500—800 cm^{-1}, most frequencies are observed commonly in the infrared and Raman spectra, although a few infrared frequencies are not observed in the Raman effect (no Raman lines have been reported below 800 cm^{-1} possibly because of the background scattering). It may be concluded that in the crystalline state, ethylene glycol molecules are not in a centrosymmetrical conformation.

The infrared spectrum of $HOCH_2CH_2OH$ in the crystalline state is similar to that in the liquid state, except for the bands primarily associated with the O–H groups. The bands due to the O–H groups in the crystalline state are observed at 3225, 737 and 689 cm^{-1} which correspond to the liquid bands at 3353 and 650 cm^{-1}. Since in the crystalline state the hydrogen bonds become stronger, the band due to the O–H stretching mode shifts to lower frequency whereas the band due to the O–H torsional mode shifts to higher frequency.

The upward shift (liquid→crystal) of the O–H torsional frequency is as great as 10%; much greater than the downward shift (~4%) of the O–H stretching frequency. Previously,[8] the O–H torsional bands of the crystal at 737 and 689 cm^{-1} have been assigned to the CH_2 rocking modes of the gauche and trans forms, respectively. However, these assignments are now revised definitely since these bands disappear on *O*-deuteration in the crystalline state as well as in the liquid state.

For ethylene glycol-d_2, $DOCH_2CH_2OD$, the infrared frequencies in the liquid and crystalline states are listed together in Table 2. The liquid band at 2475 cm^{-1} and the crystal band at 2405 cm^{-1} are due to the O–D stretching mode. In the region 600—400 cm^{-1}, an ill-defined peak is observed at about 465 cm^{-1} for liquid $DOCH_2CH_2OD$. This is primarily due to the O–D torsional mode. A peak is also observed at 520 cm^{-1}. For crystal, three main peaks are observed at 551, 527 and 491 cm^{-1}. These peaks arise from the O–D torsional and skeletal deformation modes.

For $HOCH_2CH_2OH$, the number of the bands observed in the region 1500—800 cm^{-1} is eleven for the liquid and crystalline states. This number is nearly equal to the number of the bands (thirteen) expected from the normal coordinate treatment for a model without center of symmetry. As mentioned previously, the relative band intensities do not vary with temperature in the liquid state. From these facts, it may be confirmed that ethylene glycol takes only the gauche conformation as to the C–C bond in the liquid state. Also it may be concluded now that ethylene glycol molecules take the gauche form in the crystalline state.

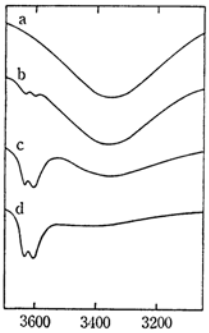

Fig. 3. Infrared spectra of ethylene glycol, $HOCH_2CH_2OH$, in the liquid state and in carbon tetrachloride solutions.
a liquid; b saturated solution; c 1/10 saturated solution; d 1/50 saturated solution

Hydrogen Bonds

The hydroxyl groups of ethylene glycol are naturally expected to form hydrogen bonds. For studying the nature of these hydrogen bonds, the infrared spectra in the region 4000—3000 cm^{-1} were measured on the carbon tetrachloride solutions of $HOCH_2CH_2OH$. The bands due to the O–H stretching modes are sensitive to the hydrogen bonds[14]; the band maxima shift to lower frequencies, and the band widths and peak intensities increase on hydrogen-bond formation.

Previously, the infrared O–H stretching bands of the carbon tetrachloride solutions of ethylene glycol have been observed at 3644 and 3612 cm^{-1},[15] at 3655 and 3619 cm^{-1},[5] and at 3637 and 3604 cm^{-1}.[10] Recently, Krueger and Mettee[16] have investigated the temperature dependence of the O–H stretching bands of ethylene glycol in the dilute carbon tetrachloride solution. They have observed bands at 3644 and 3610 cm^{-1} at room temperature and at 3644, 3614 and 3604 cm^{-1} at $-15°C$.

In the present study, the carbon tetrachloride solution was diluted stepwise to one-fiftieth of the saturated one. The saturated solution was prepared by mixing ethylene glycol with carbon tetrachloride over heating, since the solubility is very small. Infrared measurements were made with lithium fluoride optics at room temperature. The absorption curves are shown in Fig. 3.

In the liquid state only a broad band is observed at 3353 cm^{-1}. For the saturated solution, two weak bands appear at 3635 and 3604 cm^{-1}. As the solution is diluted, the band at 3353 cm^{-1} becomes weaker and shifts to higher frequency, whereas the bands at 3635 and 3604 cm^{-1} become stronger. For the solute concentration lower than one-tenth of the saturated solution, the band at 3353 cm^{-1} of the pure liquid shifts to 3370—3450 cm^{-1} and is considerably weak and broad, while the higher frequency bands are strong and sharp. Since the band intensity decreases at lower concentrations, the band at 3353 cm^{-1} is clearly due to the O–H group which forms the intermolecular hydrogen bond. On the other hand, the intensity ratio of the bands [3635 cm^{-1}/3604 cm^{-1}] does not vary with dilution. This observation indicates that these two bands arise from the monomeric species. The lower frequency band at 3604 cm^{-1} may be assigned to the O–H group which forms the intramolecular hydrogen bond and the higher frequency band at 3635 cm^{-1} may be assigned to the free O–H group.

Accordingly, in the dilute solution monomeric ethylene glycol takes, at least in part, the molecular conformation which forms the intramolecular hydrogen bond; the likely models are TGG′ and GGG′ (see Fig. 4), where, for example, TGG′ implies that the internal rotation forms about the sequence of the bonds $HO–CH_2–CH_2–OH$ are trans, gauche and gauche′ (the mirror image of the gauche). On the other hand, in the liquid state each of the two hydroxyl groups of the molecule forms the intermolecular hydrogen bonds rather than the intramolecular hydrogen bond. The likely models which have the gauche C–C bonds are TGT, TGG and GGG (see Fig. 4).

Normal Coordinate Treatment

For the vibrational analyses of the liquid bands of ethylene glycol, the normal vibrations of the TGT, TGG and GGG models were treated by Wilson's ***GF*** matrix method.[17] A NEAC 2101 digital computer (Nippon Electric Company, Ltd., Tokyo) was used for the numerical computations. The TGT and GGG models belong to

14) D. Hadzi (Ed.), "Hydrogen Bonding," Pergamon Press, London (1959).
15) L. P. Kuhn, *J. Am. Chem. Soc.*, **74**, 2492 (1952).
16) P. J. Krueger and H. D. Mettee, *J. Mol. Spectroscopy*, **18**, 131 (1965).
17) E. B. Wilson, *J. Chem. Phys.*, **7**, 1047 (1939); **9**, 76 (1941).

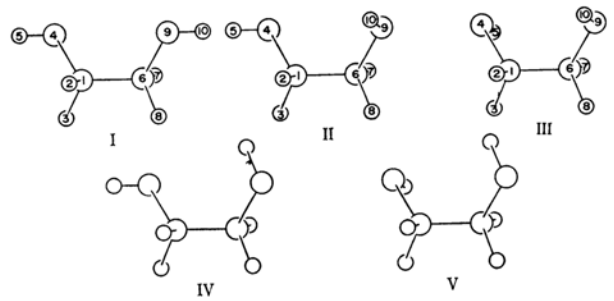

Fig. 4. Models of ethylene glycol molecule. The numbers indicate the indices used for the normal coordinate treatments.
I TGT; II TGG; III GGG; IV TGG'; V GGG'

the point group C_2 and the normal vibrations are classified into the A and B species (both infrared and Raman active), symmetric and antisymmetric, respectively, with respect to the twofold axis intersecting the C–C bond. On the other hand, the TGG model has no symmetry element except for the identity operation. This model belongs to the point group C_1, and all the vibrations are infrared and Raman active. The numbers of the vibrations are thirteen and eleven for the A and B species, respectively, of the point group C_2, and twenty-four for the C_1 group. In the region 1500—800 cm^{-1}, the expected number of the vibrations for each of these three models is thirteen (eight methylene deformation, one C–C stretching, two C–O stretching, and two O–H in-plane bending vibrations).

The indices of the carbon, oxygen and hydrogen atoms are shown in Fig. 4. The bond stretching (Δr), bond angle bending ($\Delta\phi$), and internal rotation coordinates (Δt) were used as the internal coordinates. For the calculation of the $\boldsymbol{G}$ matrices, the bond lengths of r(C–C)=1.54 Å, r(C–O)=1.43 Å, r(C–H)=1.09 Å and r(O–H)=0.97 Å and the tetrahedral bond angles ($\phi=109°28'$) were used. The internal rotation angles about the bonds HO–CH_2–CH_2–OH were taken as 180°, 60° and 180°, respectively, for the TGT model, 60°, 60° and 60° for the GGG model, and 180°, 60° and 60° for the TGG model.

In deriving the $\boldsymbol{F}$ matrix, the modified Urey-Bradley force field[18] was used:

$$\begin{aligned}2V = {} & 2V_{\mathrm{UBFF}} \\ & + Y_{\mathrm{CC}}(\Delta t_{1,6})^2 + Y_{\mathrm{CO}}[(\Delta t_{1,4})^2 + (\Delta t_{6,9})^2] \\ & + 2p[(\Delta r_{1,2})(\Delta r_{1,3}) + (\Delta r_{6,7})(\Delta r_{6,8})] \\ & + 2l[(\Delta\phi_{6,1,2})(\Delta\phi_{4,1,2}) + (\Delta\phi_{6,1,3})(\Delta\phi_{4,1,3}) \\ & \quad + (\Delta\phi_{1,6,7})(\Delta\phi_{9,6,7}) + (\Delta\phi_{1,6,8})(\Delta\phi_{9,6,8}) \\ & \quad - (\Delta\phi_{6,1,2})(\Delta\phi_{6,1,3}) - (\Delta\phi_{4,1,2})(\Delta\phi_{4,1,3}) \\ & \quad - (\Delta\phi_{1,6,7})(\Delta\phi_{1,6,8}) - (\Delta\phi_{9,6,7})(\Delta\phi_{9,6,8})] \\ & + 2T(\Delta\phi_{6,1,2})(\Delta\phi_{1,6,7}),\end{aligned}$$

where V_{UBFF} is the Urey-Bradley force field.[19,20] The initial set of the force constants were transferred from those of polyethylene,[21] methyl alcohol,[22] ethyl alcohol,[22] cyclohexane,[23] polypropylene,[24] polyethylene glycol,[25] and ethane.[26] Some of them were adjusted so that the calculated frequencies agree better with the observed ones for these models. The force constants are given in Table 3. Making use of these constants, the frequencies were calculated for the TGT, TGG and GGG models as shown in Tables 4—8. The potential energy distributions[27] (PED) were

Table 3. Potential constants[a] of ethylene glycol

K_{CH}	4.03	H_{OCH}	0.25	κ	0.08
K_{CC}	2.00	H_{COH}	0.38	Y_{CC}	0.18
K_{CO}	2.90	F_{HCC}	0.48	Y_{CO}	0.18
K_{OH}	6.10	F_{CCO}	0.28	p	−0.15
H_{HCC}	0.20	F_{HCH}	0.20	l	0.05
H_{CCO}	0.35	F_{OCH}	0.67	T	0.18
H_{HCH}	0.33	F_{COH}	0.76		

a) K, stretching constant (mdyn/Å); H, bending constant (mdyn/Å); F, repulsion constant (mdyn/Å); $F'=-F/10$; κ, intramolecular tension (mdyn·Å); Y, internal rotation constant (mdyn·Å); p, C–H stretching-interaction constant (mdyn·Å); l, C–C–H and O–C–H angle-interaction constant (mdyn·Å); and T, trans-coupling constant (mdyn·Å).

18) T. Shimanouchi, *Pure Appl. Chem.*, **7**, 131 (1963).
19) H. C. Urey and C. A. Bradley, *Phys. Rev.*, **38**, 1969 (1931).
20) T. Shimanouchi, *J. Chem. Phys.*, **17**, 245, 734, 848 (1949).
21) M. Tasumi, T. Shimanouchi and T. Miyazawa, *J. Mol. Spectroscopy*, **11**, 422 (1963).
22) C. Tanaka, Symposium on Infrared and Raman Spectra, Tokyo, November, 1964.
23) H. Takahashi, T. Shimanouchi, K. Fukushima and T. Miyazawa, *J. Mol. Spectroscopy*, **13**, 43 (1964).
24) T. Miyazawa and Y. Ideguchi, This Bulletin, **37**, 1065 (1964).
25) T. Miyazawa, K. Fukushima and Y. Ideguchi, *J. Chem. Phys.*, **37**, 2764 (1962).
26) H. Takahashi and T. Shimanouchi, Symposium on Molecular Structure, Sendai, October, 1963.
27) Y. Morino and K. Kuchitsu, *J. Chem. Phys.*, **20**, 1809 (1952); I. Nakagawa, *Nippon Kagaku Zassi (J. Chem. Soc. Japan, Pure Chem. Sect.)*, **74**, 243 (1953).

TABLE 4. THE OBSERVED AND CALCULATED FREQUENCIES (IN cm^{-1}) AND POTENTIAL ENERGY DISTRIBUTIONS[a] (IN %) OF ETHYLENE GLYCOL, $HOCH_2CH_2OH$, IN THE LIQUID STATE

$\nu_{obs.}$	TGT		TGG		GGG	
	$\nu_{calcd.}$	PED	$\nu_{calcd.}$	PED	$\nu_{calcd.}$	PED
1459 (m)	1457 B	bend 72	1463	bend 74	1464 A	bend 76
	1453 A	bend 80	1455	bend 77	1462 B	bend 77
1414 (m)	1450 A	δ_{COH} 39, wag 28	1416	δ_{COH} 47, wag 21	1405 A	δ_{COH} 32, wag 25
1392 (sh)	1417 B	δ_{COH} 57	1387	δ_{COH} 65	1373 B	δ_{COH} 80
1370 (m)	1336 A	δ_{COH} 38, twist 34, wag 17	1347	wag 42, twist 32, δ_{COH} 18	1365 A	wag 36, δ_{COH} 35, twist 20
1333 (m)	1281 B	wag 33, δ_{COH} 33, twist 21	1302	wag 41, δ_{COH} 23, twist 20	1330 B	wag 69, twist 11
1255 (w)	1258 A	twist 52, wag 28	1253	twist 51, wag 43	1266 A	twist 60, wag 30
1205 (w)	1218 B	twist 60, wag 18	1211	twist 61, wag 19	1203 B	twist 68, wag 11
1087 (s)	1150 A	rock 63	1132	rock 57	1115 A	rock 59
1062 (s)[b]	1062 B	r_{CO} 52, rock 22	1062	r_{CO} 55, rock 21	1063 B	r_{CO} 59, rock 19
1043 (s)	1016 A	r_{CO} 52, r_{CC} 31	982	r_{CO} 51, r_{CC} 27	1025 A	r_{CC} 45, r_{CO} 44
883 (s)	912 B	rock 36, r_{CO} 30	901	rock 40, r_{CO} 24	888 B	rock 46, r_{CO} 24
862 (s)	864 A	r_{CC} 50, r_{CO} 28	868	r_{CC} 60, r_{CO} 17	879 A	r_{CC} 39, r_{CO} 38
650 (s)	617 A	t_{CO} 87	646	t_{CO} 74	650 B	t_{CO} 63
	597 B	t_{CO} 63	606	t_{CO} 74	638 A	t_{CO} 90
517 (m)	476 B	δ_{CCO} 65	465	δ_{CCO} 62	454 B	δ_{CCO} 62
345 (w)	321 A	δ_{CCO} 71	322	δ_{CCO} 72	322 A	δ_{CCO} 77
	174 A	t_{CC} 77	169	t_{CC} 77	165 A	t_{CC} 81

a) bend, wag, twist and rock: bending, wagging, twisting and rocking modes of methylene group, respectively; δ: bending mode; r: stretching mode; and t: internal rotation mode.
b) Raman line.

TABLE 5. THE OBSERVED AND CALCULATED FREQUENCIES (IN cm^{-1}) AND POTENTIAL ENERGY DISTRIBUTIONS[a] (IN %) OF ETHYLENE GLYCOL-d_2, $DOCH_2CH_2OD$, IN THE LIQUID STATE

$\nu_{obs.}$	TGT		TGG		GGG	
	$\nu_{calcd.}$	PED	$\nu_{calcd.}$	PED	$\nu_{calcd.}$	PED
1460 (m)	1455 B	bend 82	1455	bend 83	1456 B	bend 83
	1452 A	bend 94	1452	bend 90	1455 A	bend 93
1390 (m)	1399 A	wag 63, twist 16	1365	wag 53, twist 27	1386 A	wag 62, twist 20
1371 (m)	1345 B	wag 68	1337	wag 67	1330 B	wag 68
1279 (w)	1271 A	twist 72, wag 17	1266	twist 58, wag 22	1272 A	twist 67, wag 15
1247 (w)	1225 B	twist 79	1231	twist 69	1236 B	twist 65
1155 (sh)	1170 A	rock 61	1171	rock 46, wag 18	1194 A	rock 46, wag 18
1085 (s)	1094 A	r_{CC} 34, δ_{COD} 26, r_{CO} 20	1091	δ_{COD} 34, r_{CO} 29, rock 13	1063 B	r_{CO} 56, rock 19
1037 (s)	1089 B	r_{CO} 40, δ_{COD} 27, rock 18	1046	r_{CO} 41, r_{CC} 25, δ_{COD} 14	1045 A	r_{CO} 48, r_{CC} 33, δ_{COD} 16
985 (m)	976 B	δ_{COD} 70, r_{CO} 13	996	δ_{COD} 67, r_{CO} 19	1008 B	δ_{COD} 80
950 (sh)	976 A	r_{CO} 51, δ_{COD} 28	949	r_{CO} 49, δ_{COD} 16 rock 14	939 A	δ_{COD} 57, rock 20
877 (s)	895 B	rock 42, r_{CO} 29	879	rock 45, r_{CO} 25	868 B	rock 47, r_{CO} 24
862 (s)	803 A	r_{CC} 52, δ_{COD} 23, r_{CO} 13	826	r_{CC} 58, δ_{COD} 18	876 A	r_{CC} 39, r_{CO} 37
520 (m)	513 B	δ_{CCO} 63, t_{CO} 22	547	δ_{CCO} 47, t_{CO} 41	565 B	δ_{CCO} 48, t_{CO} 40
465 (m)	469 A	t_{CO} 87	463	t_{CO} 84	488 A	t_{CO} 91
	404 B	t_{CO} 59, δ_{CCO} 19	398	t_{CO} 46, δ_{CCO} 32	380 B	t_{CO} 47, δ_{CCO} 33
340 (w)	309 A	δ_{CCO} 65	311	δ_{CCO} 64	313 A	δ_{CCO} 78
	171 A	t_{CC} 73	162	t_{CC} 77	154 A	t_{CC} 80

a) See a) of Table 4.

TABLE 6. THE OBSERVED[a] AND CALCULATED FREQUENCIES (IN cm^{-1}) AND POTENTIAL ENERGY DISTRIBUTIONS[b] (IN %) OF ETHYLENE GLYCOL-d_4, $HOCD_2CD_2OH$, IN THE LIQUID STATE

$\nu_{obs.}$	TGT		TGG		GGG	
	$\nu_{calcd.}$	PED	$\nu_{calcd.}$	PED	$\nu_{calcd.}$	PED
1379 (m)	1412 A	δ_{COH} 78	1390	δ_{COH} 88	1383 A	δ_{COH} 90
	1383 B	δ_{COH} 93	1376	δ_{COH} 90	1369 B	δ_{COH} 95
1189 (m)	1157 B	r_{CO} 39, wag 25	1158	r_{CO} 39, wag 29	1158 B	r_{CO} 40, wag 30
1120 (s)	1138 A	r_{CO} 34, wag 26	1121	r_{CO} 35, bend 21, wag 19	1158 A	wag 39, r_{CO} 26, r_{CC} 24
1067 (m)	1069 A	bend 66	1032	bend 59	1081 A	bend 71
1057 (m)	1018 B	bend 68	1020	bend 65	1025 B	bend 69
977 (s)	959 A	rock 57, r_{CC} 17	944	rock 38, r_{CC} 22	956 A	twist 19, wag 16, rock 15
966 (s)	931 A	wag 37, r_{CO} 27	934	wag 43, r_{CO} 30	932 B	r_{CO} 39, wag 38
945 (m)	921 B	twist 59, rock 30	919	wag 28, r_{CO} 28, twist 28	921 A	rock 49, twist 23
901 (w)	913 B	wag 51, r_{CO} 33	909	twist 50, wag 21	914 A	twist 43, r_{CO} 35
	911 A	twist 61, r_{CO} 22	903	twist 35, r_{CC} 28	904 B	twist 68
760 (m)	770 A	r_{CC} 32, wag 19	790	r_{CC} 29, wag 13	766 A	r_{CC} 28, wag 21
740 (m)	756 B	t_{CO} 34, rock 25	740	rock 34, t_{CO} 29	725 B	rock 41, t_{CO} 29
	612 A	t_{CO} 81	633	t_{CO} 75	633 B	t_{CO} 52
	586 B	t_{CO} 50	596	t_{CO} 61	629 A	t_{CO} 86
	428 B	δ_{CCO} 54, rock 25	421	δ_{CCO} 55, rock 24	414 B	δ_{CCO} 55, rock 22
	293 A	δ_{CCO} 76	295	δ_{CCO} 77	297 A	δ_{CCO} 80
	161 A	t_{CC} 86	157	t_{CC} 86	153 A	t_{CC} 88

a) Ref. 13.
b) See a) of Table 4.

TABLE 7. THE OBSERVED[a] AND CALCULATED FREQUENCIES (IN cm^{-1}) AND POTENTIAL ENERGY DISTRIBUTIONS[b] (IN %) OF ETHYLENE GLYCOL-d_6, $DOCD_2CD_2OD$, IN THE LIQUID STATE

$\nu_{obs.}$	TGT		TGG		GGG	
	$\nu_{calcd.}$	PED	$\nu_{calcd.}$	PED	$\nu_{calcd.}$	PED
1233 (w)	1220 A	wag 34, r_{CC} 33	1168	wag 38, r_{CO} 34	1170 A	wag 31, r_{CO} 27
1209 (m)	1169 B	wag 41, r_{CO} 36	1152	wag 26, r_{CO} 24	1164 B	r_{CO} 39, wag 28
1121 (s)	1112 A	bend 41, r_{CO} 24	1112	δ_{COD} 42, bend 19, r_{CC} 16	1124 A	r_{CC} 33, δ_{COD} 20, bend 17
1085 (m)	1096 B	δ_{COD} 50, bend 28	1060	δ_{COD} 40, bend 18	1064 B	δ_{COD} 56, bend 15
1033 (s)	1016 A	bend 47, δ_{COD} 24	1028	bend 65	1047 A	bend 52, δ_{COD} 28
972 (s)	997 B	bend 50, r_{CO} 23, δ_{COD} 20	996	bend 41, δ_{COD} 23, r_{CO} 20	1011 B	bend 52, δ_{COD} 18
963 (s)	945 A	rock 40, r_{CO} 22, twist 18	936	rock 25, twist 19	949 A	twist 30, r_{CO} 22, wag 21
943 (m)	918 B	twist 69, rock 28	930	wag 34, r_{CO} 29, twist 23	930 B	wag 41, r_{CO} 41
	911 A	twist 53, r_{CO} 27	915	twist 52, r_{CO} 22	911 A	twist 52, r_{CO} 29
854 (m)	875 A	wag 37, δ_{COD} 29, twist 14	877	twist 36, wag 25, δ_{COD} 23	874 B	twist 56, δ_{COD} 23
	865 B	wag 49, δ_{COD} 27, r_{CO} 22	843	δ_{COD} 23, wag 23, rock 17	857 A	δ_{COD} 35, rock 35
741 (m)	745 A	r_{CC} 42, r_{CO} 15	772	r_{CC} 39, r_{CO} 17	760 A	r_{CC} 23, rock 23, r_{CO} 16
	723 B	rock 39, twist 28	713	rock 44, twist 24	703 B	rock 48, twist 22
	491 B	δ_{CCO} 47, t_{CO} 42	522	t_{CO} 55, δ_{CCO} 32	533 B	t_{CO} 55, δ_{CCO} 32
	464 A	t_{CO} 90	459	t_{CO} 89	479 A	t_{CO} 91
	381 B	t_{CO} 37, δ_{CCO} 28, rock 25	376	δ_{CCO} 38, t_{CO} 38, rock 22	362 B	δ_{CCO} 38, t_{CO} 34, rock 18
	283 A	δ_{CCO} 72	286	δ_{CCO} 73	290 A	δ_{CCO} 80
	159 A	t_{CC} 84	151	t_{CC} 85	144 A	t_{CC} 86

a) Ref. 13.
b) See a) of Table 4.

TABLE 8. THE OBSERVED AND CALCULATED FREQUENCIES (IN cm^{-1}) OF THE O-H, C-H, O-D AND C-D STRETCHING VIBRATIONS IN THE LIQUID STATE

$\nu_{obs.}$				$\nu_{calcd.}$	Assignment[b]
$(-CH_2OH)_2$	$(-CD_2OH)_2$[a]	$(-CH_2OD)_2$	$(-CD_2OD)_2$[a]		
3353 (vs)	3300 (vs)			3399	r(OH)
2941 (s)		2938 (s)		2967 B 2962 A	$r_a(CH_2)$ $r_a(CH_2)$
2876 (s)		2877 (s)		2894 B 2879 A	$r_s(CH_2)$ $r_s(CH_2)$
		2475 (vs)	2470 (vs)	2469	r(OD)
	2212 (m)		2222 (m)	2192 B 2190 A	$r_a(CD_2)$ $r_a(CD_2)$
	2110 (m) 2083 (m)		2101 (m)	2099 B 2078 A	$r_s(CD_2)$ $r_s(CD_2)$

a) Ref. 13.
b) r(OH) and r(OD): O-H and O-D stretching modes, respectively; $r_s(CH_2)$ and $r_s(CD_2)$: CH_2 and CD_2 symmetric stretching modes, respectively; and $r_a(CH_2)$ and $r_a(CD_2)$: CH_2 and CD_2 antisymmetric stretching modes, respectively.

also calculated. The frequencies of the infrared bands in the liquid state were used as the observed frequencies.

Although the frequencies calculated for the three models do not agree quite satisfactorily with the observed frequencies, general features of the vibrational spectra may be interpreted on the basis of the results of the present normal coordinate treatments. But it seems difficult to determine the most likely model which ethylene glycol takes in the liquid state. In the following sections we will discuss the vibrational spectra of ethylene glycol and its deuterated derivatives in the liquid state.

Normal Vibrations of Ethylene Glycol, $HOCH_2CH_2OH$, and Ethylene Glycol-d_2, $DOCH_2CH_2OD$

The bands observed at 1459 and 1460 cm^{-1} for $HOCH_2CH_2OH$ and $DOCH_2CH_2OD$, respectively, are assigned to the vibrations almost exclusively associated with the CH_2 bending modes and the calculated frequencies for the three models lie in the range from 1464 to 1452 cm^{-1}, uninfluenced by the conformations about the C–O bonds. This indicates the localization of the vibrational modes in the CH_2–CH_2 group.

In the region between 1440 and 1200 cm^{-1}, liquid bands of $HOCH_2CH_2OH$ are observed at 1414, 1392, 1370, 1333, 1255 and 1205 cm^{-1}. The band at 1414 cm^{-1} is due to the O–H in-plane bending mode (δ_{COH}) as coupled with the CH_2-wagging mode. The calculated frequencies are 1450, 1416 and 1405 cm^{-1} for the TGT, TGG and GGG models, respectively, although their potential energy distributions are almost the same. Apparently, the calculated frequency is lower if the C–O bonds take the gauche conformation, but the frequency is higher if the C–O bonds take the trans conformation. The peak observed as a shoulder at 1392 cm^{-1} is almost exclusively due to the O–H in-plane bending mode, while the band observed at 1370 cm^{-1} is assigned to the hybridized vibration of the O–H in-plane bending, CH_2 wagging and twisting modes. Thus the coupling of the O–H in-plane bending mode with the methylene group deformation modes complicates the spectral feature of $HOCH_2CH_2OH$ in this region. The band at 1333 cm^{-1} is primarily due to the CH_2 wagging mode, and those at 1255 and 1205 cm^{-1} arise from the CH_2 twisting mode as coupled with the wagging mode.

In the spectra of $DOCH_2CH_2OD$, four bands are expected in the region 1440—1200 cm^{-1}, but actually five bands are observed. The bands at 1390 and 1371 cm^{-1} may be assigned to the CH_2 wagging mode, and the bands at 1279 and 1247 cm^{-1} are assigned to the CH_2 twisting mode.

For $HOCH_2CH_2OH$, four infrared bands and five Raman lines are observed in the region 1100—800 cm^{-1}. These are assigned to the CH_2 rocking and skeletal stretching modes. The frequency calculated between 1150 and 1115 cm^{-1} for the three models (TGT: 1150 cm^{-1}, TGG: 1132 cm^{-1}, and GGG: 1115 cm^{-1}) is influenced by the C–O bond conformation. The infrared band at 1087 cm^{-1} and the Raman line (polarized) at 1088 cm^{-1} are assigned to this symmetric (A species) rocking vibration of the CH_2–CH_2 group. The infrared bands and the Raman lines associated with the antisymmetric (B species) rocking mode of the CH_2–CH_2 group are observed at 883 and 1062 cm^{-1}. The former band is primarily due to the rocking mode (40%) as coupled with the C–O stretching mode (25%), while the latter is primarily associated with the C–O stretching mode (55%) although the contribution of the rocking mode

(20%) is appreciable. The infrared band corresponding to the Raman line at 1062 cm^{-1} is not observed. This may be considered that the band is weak and is overlapped by the two strong bands at 1087 and 1043 cm^{-1}. The bands observed at 1043 and 862 cm^{-1} are now found to arise from the symmetric stretching mode of the O–C–C–O skeleton.

Kuroda and Kubo[7] have previously assigned the band at 883 cm^{-1} to the CH_2 rocking modes (A and B species) of the gauche CH_2–CH_2 group, and the band at 862 cm^{-1} to the CH_2 rocking mode (A_u species) of the trans CH_2–CH_2 group. On the other hand, Kanbayashi and Nukada[10] have assigned these two bands to the CH_2 rocking modes, the B and A species, respectively, of the gauche CH_2–CH_2 group, and Miyake[13] has assigned them to the A and B species CH_2 rocking vibrations, respectively, of the gauche form. However, according to the present normal coordinate treatment, the bands associated with the CH_2 rocking modes are observed at 1087 cm^{-1} for the A species and at 883 and 1062 cm^{-1} for the B species. The band at 862 cm^{-1} which has previously been assigned to the CH_2 rocking mode is actually associated with the hybridized vibration of the C–C and C–O stretching modes. The elements of the eigenvector associated with the C–C and C–O stretching coordinates of this vibration have the same sign. Therefore the molecule carries out an overall breathing mode and the polarizability is expected to change considerably. This is quite consistent with the fact that the polarized Raman line at 864 cm^{-1} is observed strongly (see Fig. 1). On the other hand, the signs of the eigenvector elements of the vibration at 1040 cm^{-1} associated with the C–C and C–O stretching coordinates are opposite each other and the observed Raman line is not strong.

The spectral feature of liquid $DOCH_2CH_2OD$ in the region 1150—800 cm^{-1} is more complicated than the case of $HOCH_2CH_2OH$, because of the coupling of the O–D in-plane bending mode (δ_{COD}) with the CH_2 rocking and skeletal stretching modes. The bands assignable to the CH_2 rocking modes are observed at 1155 and 877 cm^{-1} for the A and B species, respectively. The bands at 1085 and 1037 cm^{-1} are primarily due to the skeletal stretching modes. The medium band observed at 985 cm^{-1} is almost exclusively due to the O–D in-plane vibration. The vibration calculated at 976—939 cm^{-1} for the three models is not observed separately. However, a weak component is seen near 950 cm^{-1} on the low frequency side of the band at 985 cm^{-1}. The band at 862 cm^{-1} may be assigned to the C–C stretching mode, corresponding to the band at 862 cm^{-1} of $HOCH_2CH_2OH$.

In the frequency region below 800 cm^{-1}, the bands due to the skeletal deformation (δ_{CCO}), internal rotation (t_{CC}) and O–H or O–D torsional modes (t_{CO}) are expected. The bands observed at 517 and 520 cm^{-1} for $HOCH_2CH_2OH$ and $DOCH_2CH_2OD$, respectively, and the Raman line (depolarized) at 524 cm^{-1} for $HOCH_2CH_2OH$ are assigned to the antisymmetric (B species) C–C–O bending mode of the O–C–C–O skeleton. The weak bands at 345 and 340 cm^{-1} for $HOCH_2$-CH_2OH and $DOCH_2CH_2OD$, respectively, and the Raman line at 350 cm^{-1} for $HOCH_2CH_2OH$ are assigned to the symmetric (A species) C–C–O bending mode. In the Raman spectrum of liquid $HOCH_2CH_2OH$, a weak line (polarized) is observed at 482 cm^{-1} in company with the line at 524 cm^{-1}.

The very broad bands due to the O–H and O–D torsional modes are observed at about 650 and 465 cm^{-1} for $HOCH_2CH_2OH$ and $DOCH_2$-CH_2 OD, respectively. The antisymmetric C–C–O bending mode of $DOCH_2CH_2OD$ is coupled with the O–D torsional mode.

Normal Vibrations of Ethylene Glycol-d_4, $HOCD_2CD_2OH$, and Ethylene Glycol-d_6, $DOCD_2CD_2OD$

The infrared spectra of $HOCD_2CD_2OH$ and $DOCD_2CD_2OD$ have been measured by Miyake[13] in the region 4000—700 cm^{-1}. The bands at 1189 and 1120 cm^{-1} of $HOCD_2CD_2OH$ are assigned to the hybridized vibration of the C–O stretching and CD_2 wagging modes. The bands observed at 1233 and 1209 cm^{-1} for $DOCD_2CD_2$-OD may also be assigned to the CD_2 wagging mode as coupled with the skeletal stretching modes. The bands due to the CD_2 bending mode are observed at 1067 and 1057 cm^{-1} for $HCOD_2CD_2$-OH; their potential energy distributions are exclusively associated with this mode. For the vibrations of $DOCD_2CD_2OD$ at 1121, 1085, 1033 and 972 cm^{-1}, the CD_2 bending mode is coupled with the C–O stretching and O–D in-plane bending modes. The bands observed in the region 1000—850 cm^{-1} for both compounds arise from the hybridizations of various vibrational modes, such as the CD_2 twisting and rocking, C–O stretching, and O–D in-plane bending modes. The band observed at 760 and 740 cm^{-1} for $HOCD_2CD_2OH$ and at 741 cm^{-1} for $DOCD_2CD_2OD$ are assigned to the C–C stretching (A species) and CD_2 rocking modes (B species), as coupled with the CD_2 wagging and twisting, and O–H torsional modes. The band at 1379 cm^{-1} observed for $HOCD_2CD_2$-OH is almost exclusively associated with the O–H in-plane bending mode. On the other hand, the O–D in-plane bending mode is coupled with various modes and the bands due to this mode are found from 1100 to 850 cm^{-1}.

C–H, C–D, O–H and O–D Stretching Modes

The bands due to the C–H and C–D stretching modes and the O–H and O–D stretching modes are expected in the region 3000—2000 cm^{-1}. The bands at 2941 and 2938 cm^{-1} of $HOCH_2CH_2OH$ and $DOCH_2CH_2OD$, respectively, are assigned to the CH_2 antisymmetric stretching mode and the bands at 2876 and 2877 cm^{-1} to the symmetric stretching mode.

The bands at 2212 and 2222 cm^{-1} of $HOCD_2CD_2OH$ and $DOCD_2CD_2OD$, respectively, are assigned to the CD_2 antisymmetric stretching mode and the bands at 2110 and 2083 cm^{-1}, and 2101 cm^{-1} to the symmetric stretching mode. The bands due to the O–H and O–D stretching modes are observed at 3353 and 2475 cm^{-1}, respectively, for $HOCH_2CH_2OH$ and $DOCH_2CH_2OD$. The observed frequency ratio for the CH_2 and CD_2 symmetric stretching modes is 1.37, the ratio for the CH_2 and CD_2 antisymmetric stretching modes is 1.32, and the ratio for the O–H and O–D stretching modes is 1.35. The frequency ratio for the symmetric stretching modes is found to be greater than the ratio for the antisymmetric stretching modes.